Surgical Assist Robot for the Active Navigation in the Intraoperative MRI: Hardware Design Issues

K. Chinzei N. Hata F.A. Jolesz R. Kikinis

Biomechanics Div.
Mechanical Engineering Laboratory
1-2 Namiki, Tsukuba, 305-8564 Japan
chin@mel.go.jp

Surgical Planning Lab.
Brigham and Women's Hospital
Francis St. 75, Boston, MA 02115, USA
{noby, jolesz, kikinis}@bwh.harvard.edu

Abstract

A magnetic resonance (MR) compatible surgical assistance robot system, designed to aid minimally invasive surgical techniques, such as positioning and directing a catheter or a laser pointer, has been built and is under preclinical evaluation.

Two specific issues arise in the MR environment: (i) the reduced space in which to place the robot; and (ii) the MR compatibility. The main mechanical body is located above the head of surgeon, with two rigid, hanging arms that reach into the workspace. This novel configuration contributes to a small occupancy in the workspace and to the MR compatibility. The robot is also carefully designed for safety and sterilization issues. Details of the kinematics and the design of the robot are given, and the MR compatibility is examined. This shows that the robot has no adverse effect on the imaging, even when it is in motion.

1 Introduction

Modern surgery requires 'pin-point' accuracy to approach a target lesion in a minimally-invasive manner. This requires the following of a pre-operatively determined trajectory with 3D numerical coordinate values, and a corresponding ability to monitor the process.

Surgical assist robots and manipulators are gradually developing their market niche as useful tools, because of their excellent precision, flexible operation, and the possibility of using them in telesurgery, etc. [1, 2, 3, 4]. With the exception of manual manipulators, which are controlled by human operators, the surgical assist robots require trajectory planning, which, in practice, relies upon preoperative images. If the target organ is deformable, then the trajectory will need to be intraoperatively updated, according to the magnitude of the deformation.

Magnetic resonance imaging (MRI) is a tomographic scanning system that has an excellent soft tissue discrimination, and a well-defined 3D coordinate reference. An intraoperative MR scanner (Signa SP/i, GE Medical Systems, Milwaukee, WI, 0.5 Tesla), has been designed to bring the power of MRI to the operating theater [5]. It has a pair of donut-shaped magnets, aligned with parallel faces, and a 560 mm air gap. Two surgeons are able to stand in the gap to access the patient. In the six years to February 2000, the author's institute has recorded more than 500 cases of the use of the intraoperative MR scanner [6, 7].

The use of MR to guide a surgical robot is promising, as it can update the trajectory based on the intraoperative images obtained. However, an MR scanner is a highly restrictive environment for foreign objects, and, in particular, for robots. It has a strong, static magnetic field, and a temporal, spatially-varying gradient magnetic field. The magnitude of the static magnetic field of the intraoperative MR scanner is 0.5 Tesla. The precision of this magnetic field needs to be maintained in the order of a few parts per million (ppm). To excite nucreus, the RF radio wave (or RF pulse) corresponding to the resonance frequency is applied. Its power can reach the order of a few kilowatts. For hydrogen nucreus ($^1_1$H) in a field of 0.5 Tesla, the resonance frequency is approximately 21.3 MHz. The observed resonance signal is quite weak, so that the receiver gain needs to be in the region 60–80 dB, and noise from nearby electrical equipment can easily mask it.

In practice, ferric materials and noisy electric circuits (in particular digital circuits) cannot be present or function in the MR scanner room without incorporating special design principles. Schenck, for example,

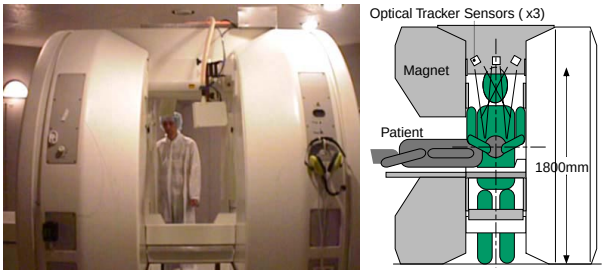

Figure 1: The intraoperative MR scanner (left), and its profile with a patient and a surgeon (right). A surgeon of medium height is represented. The three visual sensors of the tracking device are located in the central bridge between the two magnets. The sensor field of vision has to be clear during operation.

has reviewed the magnetic compatibility of MRI systems [8], and GE Medical Systems have issued comprehensive and practical guidelines regarding MR safety and compatibility [9]. Masamune has developed an MR compatible manipulator with six degrees-of-freedom [10]. This was mainly built from plastics, and so suffered from a lack in rigidity. We have previously investigated the MR compatibility of mechanical devices, summarizing MR compatible techniques, and, further, showed how it was possible to build a precise MR compatible mechanism [11].

In this paper, we demonstrate the unique configuration of a novel robotic system for MR guided surgery. The main topic of this paper is on the hardware design issues: the hardware design solutions needed to fit the unique configuration of the intraoperative MRI, and the hardware design solutions for MR compatibility. In Section 3, we introduce the configuration of the robot. This is analyzed in detail in Section 4, as well as showing the validation of the MR compatibility.

2 Requirements and Specifications

In this section, we define the requirements of robot-assisted procedures under MR guidance, and, from these, derive the specification of the robot.

2.1 Goals of MR Guided Robotic Assist

The purpose of robotic assistance under MR guidance is to actively navigate minimally invasive procedures, such as catheter [1] insertion, with 'pin-point' accuracy. Intraoperative images serve as the source of trajectory revisions. In the above example, the robot would hold the catheter for the surgeon. The robot would position, and direct the catheter. Technically, the robot can perform the insertion; however, our current plan reserves this task for the surgeon, for ethical and legal reasons.

Our intention is to introduce robotic assistance to enhance the surgeons' performance, and not to eject them from the surgical field. Therefore, the robot must coexist with the surgeons.

[1] Catheter is a hollow needle to guide other devices such as an endoscope, a fiber optic, and a suction tube.

2.2 MR Environment-Specific Restrictions

In addition to the standard requirements of surgical robots, such as safety and sterilization issues, there are two specific restrictions in the MR environment.

Layout: The robot must coexist with the surgeon. However, when the surgeon is operating on the patient, little space remains for the robot (Fig. 1, right). In addition, the occlusion of the sensors of the optical tracker should be minimal.

MR compatibility: To enable the real-time tracking of the target position, the robot should be able to maneuver, even during imaging. The robot motion should not have any adverse effect on the image, and the robot, in turn, should not be affected by the imaging. In other words, the robot should be MR compatible. A descriptive definition of MR compatibility can be found in [9]. In addition, the robot should be MR safe. The MR safety of the robot requires that the machine should not unintentionally move from any magnetic attraction, and no electromagnetic side-effects (e.g., the leakage of, and the heating by, eddy current and RF pulses) should occur.

3 Materials and Methods

3.1 Configuration and Kinematics

To clear the workspace for the surgeon, the robot is placed away from the surgical field. This also contributes to a better MR compatibility. However, there is a trade-off between space-saving and mechanical performance. Keeping the robot at a distance can decrease the precision and the dynamic response.

Our robot has a configuration in which the mechanical main body is positioned above the head of the surgeon, and the two rigid arms hang down to reach the workspace (Fig. 2 left).

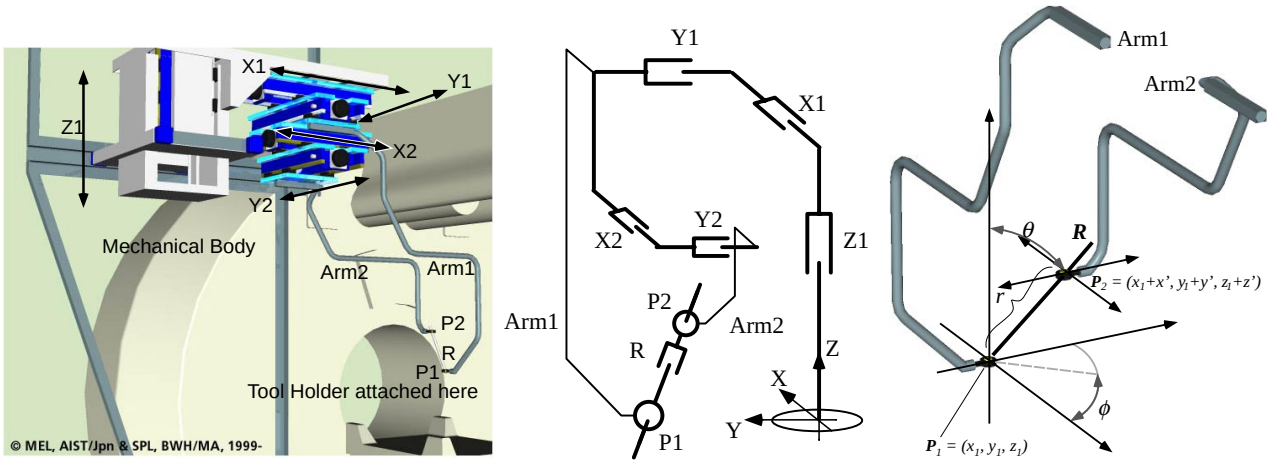

Figure 2: The configuration of the robot. The mechanical body has five axes in total. All axes are driven by linear motion mechanisms. Two rigid arms hang from the body. Arm 1 is actuated by X1, Y1, and Z1. Arm 2 is actuated by X2 and Y2. The ends of the arms are linked by two spherical joints, P1 and P2, and the sliding bar, R. A tool holder is attached at P1. P1 moves in 3D space, and P2 moves in a 2D plane relative to P1. The direction of the line segment between P1 and P2, $(= r)$, is determined by the position of P2. Mathematically, this is a polar coordinate system with origin at P1.

Five degrees-of-freedom are sufficient to position and direct a catheter or a laser pointer, because these instruments are axisymmetric. All the actuated axes operate by linear motion mechanisms (i.e., there are no rotational joints). The first three axes (X1, Y1, Z1) drive a rigid arm (Arm1), and the two remaining axes (X2, Y2), drive a second rigid arm (Arm2). These arms are linked together by two pivot joints (P1, P2), and a sliding joint, R. P1 defines a point in the 3D coordinate system, and P2 travels in a 2D plane relative to P1. (Fig. 2).

The tool holder is attached to P1. For simplicity, we assume here that the position of the tool holder is P1, and its direction is parallel to that of R. The position and direction of the tool holder is described in polar coordinates with the origin at P1 (Eq. 1).

$$\begin{aligned} x' &= r\cos\phi\sin\theta \\ y' &= r\sin\phi\sin\theta \\ z' &= r\cos\theta \end{aligned} \tag{1}$$

where P1 $= (x_1, y_1, z_1)$, P2 $= (x_1 + x', y_1 + y', z_1 + z')$, $(z'$ is a constant), $r^2 = x'^2 + y'^2 + z'^2$. The direction (ϕ, θ) is determined only by the relative position of P2 to P1, (x', y', z'). Therefore, the direction is independent of P1. When the tool holder is attached to P1 and offset, its position is dependent on (ϕ, θ). Denoting this offset of the end effector from P1 as $[x_{e0}, y_{e0}, z_{e0}]$ when $(\phi, \theta) = (0, 0)$, the offset of the end effector $[x_e, y_e, z_e]$ is given by the following equation (Eq. 2).

$$\begin{bmatrix} x_e \\ y_e \\ z_e \end{bmatrix} = \begin{bmatrix} \cos\phi\cos\theta & -\sin\phi & \cos\phi\sin\theta \\ \sin\phi\cos\theta & \cos\phi & \sin\phi\sin\theta \\ -\sin\theta & 0 & \cos\theta \end{bmatrix} \begin{bmatrix} x_{e0} \\ y_{e0} \\ z_{e0} \end{bmatrix} \tag{2}$$

3.2 MR Compatibility- Design and Evaluation

All parts of the robot were made from paramagnetic materials such as titanium alloy and plastics. Non-magnetic ultrasonic motors, USR60–S3N (Shinsei Kogyo Corp., Tokyo, Japan), directly drive the ball screws. The maximum rotational speed of the motor is ca. 150 r.p.m., the maximum rotation and the holding torques are 0.5 and more than 0.7 Nm respectively. Each motional axis has optical position detection sensors. Optical fibers transfer the signals to optoelectronic conversion circuits located outside the scanner room, for better noise immunity.

We have investigated the loss of homogeneity of the magnetic field, and the signal-to-noise ratio (SNR) of the image. There are several possible interactions when the robot is located in, and is maneuvering in, the MR environment. The presence of, and motion of, the robot can distort, or shift, the image by decreasing the homogeneity of the magnetic field, and these can

Figure 3: The constructed robot installed with the intraoperative MRI.

also affect the image SNR. Other effects (e.g., heating and eddy current leakage) can be safely ignored by using basic isolation methods, as shown by previous workers [12].

A spherical phantom (diameter = 280 mm) was imaged using the imager. This contained $CuSO_4$ solution, which gave a delta-function shape resonance spectrum in an ideal, homogenous magnetic field. The inhomogeneity was defined by the diversity of the observed spectrum. The SNR was calculated using the following equation (Eq. 3).

$$SNR = Pcenter/SDcorner \ . \tag{3}$$

where $Pcenter$ is the mean value of the 40×40 pixel area at the center of the image, and $SDcorner$ is the standard deviation of the 40×40 pixel area in the lower right corner of the image. The sequence was the Spin Echo, TE/TR = 85/220 ms, and the receiver bandwidth was 62.5 kHz. The robot repeated a simple Y2 axis motion, which was the most adjacent axis to the imaging region. The control data were obtained by the same phantom without the robot.

4 Results

The construction of the first version of the robot system has been completed, and the system is currently in the software tuning, and preclinical evaluation stages.

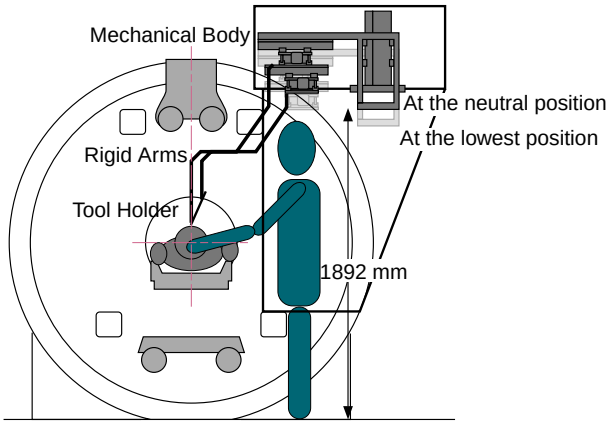

Figure 4: Profile of the workspace. The moving part clears the workspace for the surgeon.

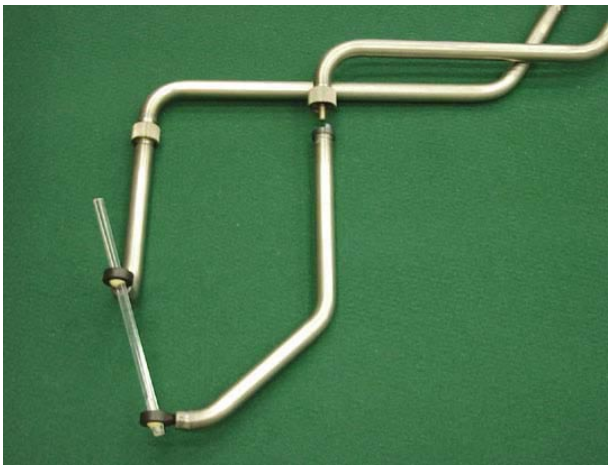

Figure 5: The rigid arms and the pivotal joints. The arms can be divided into parts small enough to be autoclaved.

4.1 Configuration

Figure 3 shows the constructed robot installed with the intraoperative MRI.

When the vertical axis is at its lowest position, the moving part's minimum height (apart from the arms, and part of the vertical axis, Z1) is 1892 mm from the floor (the bottom of the Y2 axis, Fig. 4). The arms are bent so that they do not collide with the scanner. Each arm can be divided into three pieces (Fig. 5). The end pieces can fit into an autoclave tray that is currently used in the authors' hospital. This design also allows the selection of a suitable arm shape, according to the procedure.

Table 1: Obtained inhomogeneity values. The smaller value is the greater homogeneity.

Inhomogeneity	(ppm)
Spherical phantom, without robot (baseline)	0.45
Spherical phantom, with moving robot	0.53
Spherical phantom, with an 'MR compatible' Mayfield stereotactic frame	0.9
Human volunteer	ca. 1.4

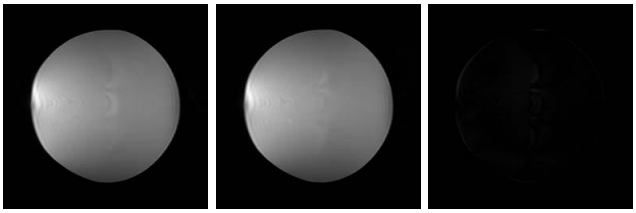

Figure 6: Images of the spherical phantom when the robot was not installed (left) and when one axis of the robot was in motion (center). The subtraction of these images showed no shift (right).

4.2 MR Compatibility

The magnetic field inhomogeneity values are listed in Table 1. The inhomogeneity value was observed to be 0.53 when the robot was in motion. This is better than that of a clinically-used stereotactic frame, or of the human body itself. The effect on the homogeneity of the magnetic field was negligible.

The SNR loss was 1.6 to 1.8%. As an SNR loss is acceptable up to 10%, the observed value was in the negligible range. Figure 6 shows an image of the spherical phantom with, and without, the robot.

5 Discussion

The main body of the robot is located above the surgeon. It is composed of linear motion mechanisms only, and the end effector is attached at the end of two long, rigid arms through pivotal joints. This configuration of the robot possesses several advantages:

- The mechanical body is positioned 1–2 m away from the center of the imaging volume. At this distance, the magnetic susceptibility and the current of the motors have little impact on the MR compatibility.

- The arms are slender, which is valuable in the narrow MRI operating field. The conventional wrist-type robots have rotational joints, which can magnify the error at the end of a long arm. In addition, unless employing complicated wires or a similar mechanism, a joint actuator must sustain the weight of the other actuators at the effector end. These would result in thicker and bulkier arms than the current design.

- The kinematics and inverse kinematics are simple. Therefore, when the surgeon wants to move the end effector, he or she can predict the change in the posture.

- The arms and the end effector are detachable, exchangeable, and sterilizable.

The configuration has a disadvantage in that the long arms decrease the rigidity. This limits the robot to accepting lightweight end effectors, and it does not provide for a dexterous (and heavy) hand. However, the robot is not intended to behave like a human surgeon. Rather, it should perform something that human surgeons do not perform very well. Needle insertion is one such action, and is a common procedure in many minimally invasive operations.

5.1 Safety and Sterilization Issues

The surgeon is responsible for avoiding collisions, as there is no reliable, universal, automated technique to overcome this problem. Therefore, the simplicity of the mechanism is an important factor in helping the surgeon to understand, and anticipate, the subsequent motion of the robot. With the polar coordinate system, it is relatively easy to guess the motion and posture of the robot from a given numerical coordinate values and the direction angles.

Because of the strong holding torque of the ultrasonic motor, the robot maintains its posture even in the event of a power break. As the sensors used are optical, they already have electromagnetic immunity, and the optoelectronic conversion circuits are placed outside the scanner room for enhanced noise immunity from the strong RF pulses.

As shown in Figure 5, the rigid arms can be divided into shorter pieces, and the end piece can be autoclaved. The other parts of the arms and the mechanical body can be draped. EOG sterilization can be applied to the pivotal joints and the other plastics parts.

6 Conclusion

An MR compatible surgical assist robot is in the preclinical evaluation stage. It is designed to cooperate with, and to assist, surgeons to perform minimally invasive procedures, such as catheter biopsies. It can position, and direct a catheter, a laser pointer, or any other lightweight tool.

To be MR compatible, and to fit into the restricted space of the intraoperative MRI, the robot has a unique configuration. All the mechanical axes are located above the surgeon's head. Two rigid arms extend to the workspace, and the end effector is attached to the ends of the arms. The end effector is simple, and therefore do not occupy much of the valuable space in the surgical field. The robot is made from paramagnetic materials, and is driven by non-magnetic ultrasonic motors. The electrical circuits, including those of the sensors, are remotely isolated outside the MR scanner room for noise immunity.

The robot showed an excellent MR compatibility. Its motion did not appear to have any adverse effect on the imaging, and the robot was not affected by the imaging process. The authors have not experienced any heating during the imaging, as has been previously reported. Likewise, any other adverse side effects can be safely neglected.

Acknowledgments

In Japan, the project has been funded by MITI, "Study of Open MRI-Guided Diagnosis/Treatment Concurrent System", and "Research on MR compatible active holder for surgical assistance".

In the USA, the project has been funded by NSF Engineering Research Laboratory "Computer Integrated Surgical Systems and Technology" #9731748, and "MR Guided Therapy" 3P01CA67165–03S1 funded by NIH.

The authors would gracefully acknowledge the assists of Mr. Dan Kacher, Mr. Oliver Schorr, Dr. Toshikatsu Washio to conduct the experiments.

References

[1] N. Villotte, D. Glauser, P. Flury, et.al., "Conception of Stereotactic Instruments for the Neurosurgical Robot Minerva," proc *IEEE ICRA*, pp. 1089–90, 1992.

[2] R.H. Taylor, B.D. Mitterlstadt, H.A. Paul, et.al., "An Image-Directed Robotic System for Precise Orthopedic Surgery," In R.H. Taylor, et.al. (eds) "Computer-Integrated Surgery : Technology and Clinical Applications," MIT Press, pp. 379–95, 1995.

[3] J.M. Sackier, Y. Wang, "Robotically Assisted Laparoscopic Surgery: From Concept to Development," In R.H. Taylor, et.al. (eds) "Computer-Integrated Surgery : Technology and Clinical Applications," MIT Press, pp. 577–80, 1995.

[4] P.S. Schenker, H. Das, T.R. Ohm, "A New Robot for High Dexterity Microsurgery," proc *CVRMed95*, Lecture Notes Computer Science, Vol. 905, Springer-Verlag, pp. 115–22, 1995.

[5] J.F. Schenck, F.A. Jolesz, P.B. Roemer, et. al., "Superconducting Open-Configuration MR Imaging System for Image-Guided Therapy," *Radiology*, Vol. 195, No. 3, pp. 805–14, 1995.

[6] S.G. Silverman, B.D. Collick, M.R. Figueira, et.al., "Interactive MR-guided biopsy in an open-configuration MR imaging system," *Radiology*, Vol. 197, pp. 175–81, 1995.

[7] N. Hata, P.R. Morrison, J. Kettenbach, et.al., "Computer-assisted Intra-Operative Magnetic Resonance Imaging Monitoring of Interstitial Laser Therapy in the Brain: A Case Report," *J Biomedical Optics*, Vol. 3 No. 3 pp. 304–11, 1998.

[8] J.F. Schenck, "The role of magnetic susceptibility in magnetic resonance imaging: MRI magnetic compatibility of the first and second kinds," *Med Phys*, Vol. 23, No. 6, pp. 815–50, 1996.

[9] GE Medical Systems (ed), "MR Safety and MR Compatibility: Test Guidelines for Signa SP," www.ge.com/medical/mr/iomri/safety.htm, 1997.

[10] K. Masamune, E. Kobayashi, Y. Masutani, et.al., "Development of an MRI compatible Needle Insertion Manipulator for Stereotactic Neurosurgery," *J Image Guided Surgery*, Vol. 1, pp. 242–8, 1995.

[11] K. Chinzei, R. Kikinis, F.A. Jolesz, "MR Compatibility of Mechatronic Devices: Design Criteria," proc *MICCAI '99*, Lecture Notes in Computer Science, Vol. 1679, Springer-Verlag, pp. 1020–31, 1999.

[12] R. Buchili, P. Boesiger, D. Meier, "Heating Effects of Metallic Implants by MRI Examinations," *Magn Reson Med*, Vol. 7, pp. 255–61, 1988.